JOURNAL OF GEOPHYSICAL RESEARCH, VOL. 105, NO. D18, PAGES 22,811–22,823, SEPTEMBER 27, 2000

Path histories and timescales in stratospheric transport: Analysis of an idealized model

Timothy M. Hall

NASA Goddard Institute for Space Studies, New York

Abstract. Mean age and the age spectrum, transport diagnostics independent of photochemistry, have been put to good use diagnosing stratospheric circulation and evaluating models. These diagnostics reveal how long air took to reach a stratospheric location from the troposphere, but they provide no direct information about where the air traveled en route. I define a complement to the age spectrum to explore how stratospheric transport timescales are related to path histories. Just as one constructs the age spectrum by distributing components of an air parcel according to transit time since last tropospheric contact, one can distribute the components according to the maximum height achieved en route to the parcel. Combining the age spectrum and the "maximum path height" distribution, one has a "joint distribution" of transit time and maximum path height. These ideas are illustrated with an idealized model of stratospheric transport, as well as a general circulation model. Transport features in the idealized model that strongly affect mean age affect the distribution of maximum path heights relatively weakly, especially in midlatitudes. The mass fraction of an air parcel at r that passed above some specified height z above r is strongly constrained by the mass continuity of stratospheric regions and is only more weakly affected by the circulation. This represents a limit on the relationship between mean age and trace gases of predominantly upper stratospheric photochemistry.

1. Introduction

The mean age is a diagnostic of stratospheric transport independent of photochemistry. It represents the mean over the distribution of transit times (the age spectrum) since a stratospheric air parcel has last been in the troposphere and may be inferred from an inert tracer whose atmospheric abundance is increasing linearly [*Hall and Plumb*, 1994]. CO_2 and SF_6 are trace gases that approximately satisfy these conditions, and in recent years, measurements made from aircraft and balloons of these and other gases have been used to infer mean age [*Schmidt and Khedim*, 1991; *Boering et al.*, 1996; *Elkins et al.*, 1996; *Harnisch et al.*, 1996; *Patra et al.*, 1997], as well as the age spectrum [*Andrews et al.*, 1999; *Johnson et al.*, 1999]. Mean age observations have in turn been used to evaluate transport in stratospheric models [*Waugh et al.*, 1997; *Hall et al.*, 1999]. Many models have been found to significantly underestimate mean age [*Hall et al.*, 1999].

Although mean age is a powerful transport diagnostic, a limiting feature is that it provides no direct information on where air has been, only on how long it took to get there. One could imagine an irreducible fluid element ("particle") with a particular transit time having resided exclusively in the lower stratosphere or having traversed the upper stratosphere before reaching an air parcel under observation. (Throughout, "particle" refers to an indivisible and unobservable entity, while a "parcel" is the observable entity composed of many particles.) Although these scenarios are indistinguishable for mean age, they have very different consequences for the parcel's abundance of the many photochemically active species whose loss and production rates vary strongly with height [see *Schoeberl et al.*, 2000, Figure 1]. *Hall et al.* [1999] showed that in the lower stratosphere across a large range of models mean age was correlated with the simulated distributions of photochemically active trace gases such as total organic chlorine (Cl_y), total reactive nitrogen (NO_y), and N_2O, indicating that inaccuracies in model transport were responsible for much of the wide range in simulated lower stratospheric distributions of these gases. However, although correlation was high in the lower stratosphere, it degraded with altitude. In addition, several models that significantly underestimated mean age had more realistic distributions of N_2O. Generally, the simulations of Cl_y, NO_y, and N_2O, considered over the whole stratosphere, varied less among models than mean age. Similarly, *Li and Waugh* [1999] explored the sensitivity of mean age and stratospheric long-lived trace gas distri-

Paper number 2000JD900329.
0148-0227/00/2000JD900329$09.00

butions to transport rates in a two-dimensional (2-D) model and found significant but imperfect correlation between the gas distributions and the mean age across their set of numerical experiments. To understand better the implications of a model's underestimate of mean age and to establish the relationship between the mean age and the mixing ratios of photochemically active trace gases, one would like to have information on the path histories of the components of an air parcel, and how these histories relate to the mean age. Such information would help modelers judge how hard they should work to improve the realism of their mean age simulations.

In this paper I explore one technique to summarize path history information. Just as the age spectrum is the distribution of transit times since last tropospheric contact, one can consider the distribution of maximum heights achieved en route from the last tropospheric contact, or more generally, a joint distribution of transit times and maximum path heights. These distributions are defined in section 2 and illustrated in section 3 with a hierarchy of idealized stratospheric models and with a 3-D numerical model. I explore the relationship between the maximum path height distribution and the mean age in section 4, finding surprising insensitivity of the maximum path height distribution to transport rates that strongly affect mean age. I conclude in section 5, discussing the application of these ideas to understanding the relationship between photochemically active trace gas concentrations and mean age.

2. Maximum Path Height Distribution

To construct the age spectrum conceptually, one distributes the particles which comprise an air parcel according to their transit times since the last contact with the troposphere. In principle, the particles can be distributed by a different variable, or additional variables. Perhaps most relevant to photochemically active gases would be some measure of ultraviolet exposure integrated along a particle path, but this would necessitate assumptions about photochemical rates and overhead abundance of other gases. Since many trace gases have photochemical rates that vary rapidly with height, a natural pure transport variable is the maximum height achieved by particles en route to the observation point from the troposphere. The "maximum path height" (MPH) distribution $\mathcal{Z}(\mathbf{r},t|z)$ is defined as follows: for a parcel at position $\mathbf{r}$ at time t, $\mathcal{Z}(\mathbf{r},t|z)\delta z$ is the mass fraction of the parcel that reached a maximum height between z and $z+\delta z$ since last troposphere contact. Note that $\mathcal{Z}=0$ for $z<z_r$, where $z_r=\mathbf{r}\cdot\hat{z}$ is the height of the parcel. By construction, $\int_{z_r}^{\infty}dz'\mathcal{Z}(\mathbf{r},t|z')=1$. Similar statistical formulations have been used elsewhere, for example, to describe the penetration of radiation in biological media [*Sparling and Weiss*, 1993]. The MPH distribution and age spectrum also depend on the location and extent of the boundary region, a dependence that has been explored for the age spectrum by *Holzer and Hall* [2000]. In this paper, however, I always consider the boundary region to be the whole troposphere and suppress the boundary dependence in the notation for simplicity.

The diagnostic $\mathcal{Z}$ distributes the particles according to maximum path height, independent of the transit time. By contrast, the age spectrum G distributes the particles according to transit time, independent of the maximum path height. The two distributions may be combined by considering a distribution of maximum path heights conditioned on a particular transit time ξ or, identically, by considering the distribution of transit times conditioned on a particular maximum path height. One has the maximum path height transit time distribution or, simply, the "joint distribution" $\mathcal{P}(\mathbf{r},t|z,\xi)$ such that $\mathcal{P}\delta z\delta\xi$ is the mass fraction of the parcel at $\mathbf{r}$ and t that was last in the troposphere a time ξ to $\xi+\delta\xi$ ago and reached maximum height z to $z+\delta z$ en route. By construction, $\int_{z_r}^{\infty}dz\int_0^{\infty}d\xi\mathcal{P}=1$. The age spectrum is recovered as $G(\mathbf{r},t|\xi)=\int_{z_r}^{\infty}dz\mathcal{P}(\mathbf{r},t|z,\xi)$, and the MPH distribution as $\mathcal{Z}(\mathbf{r},t|z)=\int_0^{\infty}d\xi\mathcal{P}(\mathbf{r},t|z,\xi)$.

In practice, to obtain $\mathcal{Z}(\mathbf{r},t|z)$ in a model, one first computes the cumulative distribution $\int_{z_r}^{z}\mathcal{Z}(\mathbf{r},t|z)dz'$, the mass fraction of the parcel at $\mathbf{r}$ that has not been above z since last tropospheric contact. A tracer is defined with a tropospheric mixing ratio boundary condition (BC) of $q(0)=1$ ($Z=0$ at the tropopause) and an upper BC $q(z)=0$. In steady (or cyclostationary) state at a point $\mathbf{r}$ below z, $q(\mathbf{r},t)$ represents the fraction of the parcel at time t that has not been above z since last tropospheric contact. Redefining the tracer with an upper BC at $z+\delta z$ gives the fraction that has not been above $z+\delta z$, and the difference is $\mathcal{Z}(\mathbf{r},t|z)\delta z$, the fraction that reached between z and $z+\delta z$. If q is known analytically, than $\mathcal{Z}=dq/dz$. For a numerical model, separate tracers are defined and run to steady (or cyclostationary) state, each tracer having a unit tropospheric BC and a zero upper BC, and each corresponding to a successively increased upper BC level (e.g., increased by one model grid level). Then $\mathcal{Z}(\mathbf{r},t|z)=(q(\mathbf{r},t|z+\Delta z)-q(\mathbf{r},t|z))/\Delta z$, where Δz is the model vertical grid spacing. The recipe for the joint distribution $\mathcal{P}$ is similar, except that one computes the transient response $q(\mathbf{r},t,t')$ to the time-dependent BC $\delta(t-t')$, where δ is the Dirac delta function. The differentiation with respect to the upper BC is now performed at each time step and considered as a function of elapsed time $\xi=t-t'$, thereby resulting in a function $\mathcal{P}(\mathbf{r},t|z,\xi)$ of transit time ξ (elapsed time) and maximum path height z (upper boundary height) for the parcel at $\mathbf{r}$ and t. $\mathcal{P}$ and $\mathcal{Z}$ are also functions of the parcel position $\mathbf{r}$ and time t. The t dependence occurs because transport is, in general, not stationary. For the idealized case of stationary transport, all diagnostics are independent of t, depending only on elapsed time ξ. Note that for the upper BC at $z=\infty$, $\mathcal{P}$ reduces to the age spectrum.

3. Illustrations

In this section I illustrate the distributions defined above with an idealized model of the stratosphere, the

"tropical leaky pipe" (TLP) model. Transport features are added to the TLP model (advection, midlatitude-tropical mixing, and diffusion) one at a time to observe their impacts on the MPH and joint distributions. Subsequently, I compute the distributions in a 3-D numerical model of the stratosphere.

3.1. Tropical Leaky Pipe Model

The TLP model was defined and motivated by *Plumb* [1996] and *Neu and Plumb* [1999], its mean age distribution solved and analyzed by *Neu and Plumb* [1999], and its residence time computed by *Hall and Waugh* [2000]. Under certain limits the model permits analytic solutions for tracer distributions, useful for exploring the relationship between tracer diagnostics and transport rates. In general, the TLP model consists of three coupled 1-D diffusive-advective regions: a "tropical" region with upward advection and two "midlatitude" regions (south and north) with downward advection. Continuity and the tropical mass divergence cause a net tropical to midlatitude flux with a rate constant λ proportional to the divergence (see *Neu and Plumb* [1999]). In addition, two-way mixing occurs by allowing mixing ratio differences between the tropics and the midlatitudes to relax with a timescale τ. These features summarize the large-scale, time-averaged transport effects of the stratospheric circulation. *Hall and Waugh* [2000] have shown that the TLP model can reproduce tracer distribution features seen in numerical 2-D and 3-D simulations of stratospheric point sources. The model's free parameters have been indirectly inferred from a number of observational studies [*Grant et al.*, 1996; *Minschwaner et al.*, 1996; *Volk et al.*, 1996; *Sparling et al.*, 1997; *Hall and Waugh*, 1997b; *Mote et al.*, 1998].

The TLP equations for a tracer of mixing ratio q are

$$\frac{\partial q_T}{\partial t} + W\frac{\partial q_T}{\partial Z} - K_T e^{Z/H}\frac{\partial}{\partial Z}(e^{-Z/H}\frac{\partial q_T}{\partial Z}) = -\frac{1}{\tau}(q_T - q_M), \quad (1)$$

$$\frac{\partial q_M}{\partial t} - \alpha W\frac{\partial q_{NH}}{\partial Z} - K_M e^{Z/H}\frac{\partial}{\partial Z}(e^{-Z/H}\frac{\partial q_M}{\partial Z}) = (\lambda + \frac{\alpha}{\tau})(q_T - q_M). \quad (2)$$

The vertical coordinate Z is "equivalent height" [*Plumb*, 1996; *Neu and Plumb*, 1999], with $Z = 0$ representing the tropopause in both tropical and midlatitude regions. See *Neu and Plumb* [1999] and *Hall and Waugh* [2000] for the impact of a tropical tropopause elevated with respect to midlatitudes. In equations (1) and (2) the subscripts T and M indicate the tropical region and midlatitude region, W is the tropical vertical velocity, K is the vertical diffusivity in equivalent height coordinates, and $\alpha = M_T/(2M_M)$ is the ratio of total air mass in the tropical column to the total air mass in the midlatitude columns ($\alpha = 0.5$ corresponds to tropical edges at $\approx \pm 20°$). Air mass density is assumed to decay as $e^{-Z/H}$ with a uniform scale height H. Compared to *Neu and Plumb* [1999] and *Hall and Waugh* [2000], the northern and southern midlatitude equations are here combined into one, equation (2), as I will only consider hemispherically symmetric coefficients and boundary conditions.

The timescale τ summarizes the mixing between regions. I will often employ an alternative measure, $\epsilon = \alpha/(\tau\lambda)$, to represent the tropical-midlatitude coupling. As defined by *Neu and Plumb* [1999], ϵ is the ratio of gross "detrainment" (midlatitude-tropical flux) to net "entrainment" (tropical-midlatitude flux). The net entrainment is constrained by continuity, but the detrainment is free to vary. For the "tropical pipe" or nondetraining (no mixing), limit $\epsilon = 0$, while in the "global diffuser" (instantaneous mixing) limit, $\epsilon = \infty$. If W is uniform, then $\epsilon = H/(W\tau)$. In section 4 some effects of spatial variation in W are discussed.

3.2. Advection, No Detrainment, No Diffusion

In the simplest and least realistic case there is no mixing between the midlatitudes and tropics. This is the "tropical pipe" limit of *Plumb* [1996] in which the tropical continuity equation decouples from midlatitudes. If, in addition, one assumes no vertical diffusion ($K = 0$) and uniform vertical velocity ($\lambda = \alpha W/H$), then one finds for the age spectrum

$$G_T(Z,\xi) = \delta(\xi - Z/W), \quad (3)$$

$$G_M(Z,\xi) = \alpha_+ \frac{W}{H} e^{-\alpha_+ \frac{W}{H}(\xi - Z/W)}\,\Theta(\xi - Z/W), \quad (4)$$

where $\alpha_+ = \alpha/(1+\alpha)$ and Θ is the Heaviside function ($\Theta(\xi) = 1$ for $\xi > 0$ and zero otherwise). The tropical age spectrum is simply a delta function lagged by the advection time Z/W, as there is no mixing of older extratropical air into the tropics. The midlatitude age spectrum is composed of a range of transit times, as a midlatitude parcel is made up of air that is transported from the tropics to extratropics at different heights, then homogenized instantaneously in the TLP surf zone. This is illustrated schematically in Figure 1 . Note that no air can arrive in midlatitudes before Z/W, the time required to first travel up to Z in the tropics.

The joint distribution is

$$\mathcal{P}_T(Z,Z',\xi) = \delta(\xi - Z/W)\delta(Z' - Z), \quad (5)$$

$$\mathcal{P}_M(Z,Z',\xi) = \frac{1}{H} e^{-\alpha_+ \frac{W}{H}(\xi - Z/W)}\,\Theta(Z' - Z) \times \delta\left(\xi - \frac{Z'}{W} - \frac{(Z' - Z)}{\alpha W}\right). \quad (6)$$

One can obtain $\mathcal{Z}$ by integrating $\mathcal{P}$ over all transit times ξ to find

$$\mathcal{Z}_T(Z,Z') = \delta(Z' - Z), \quad (7)$$

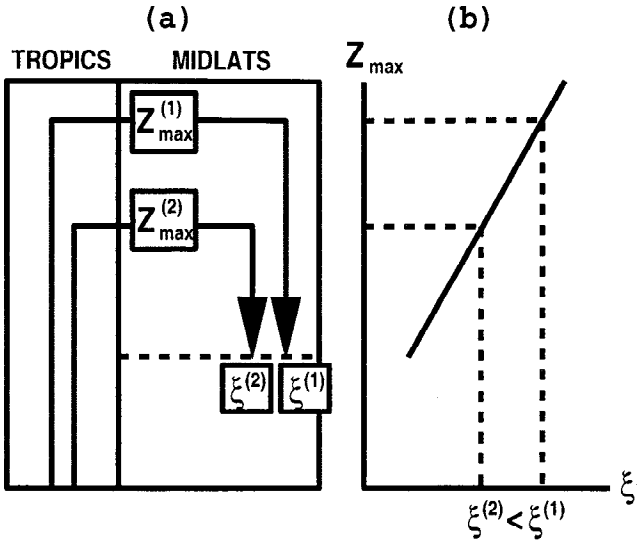

Figure 1. (a) Schematic of trajectories in the nondetraining limit. (b) Singular one-to-one relationship between transit time and maximum path height.

$$\mathcal{Z}_M(Z, Z') = \frac{1}{H} e^{-(Z'-Z)/H} \Theta(Z' - Z). \quad (8)$$

These solutions summarize the simple situation shown schematically in Figure 1. The tropical age spectrum is a delta function, as discussed above. The tropical MPH distribution is also a delta function. The only tropical transport mechanism is pure upward advection, so no air at Z has passed higher than Z itself. The midlatitude G_M and $\mathcal{Z}_M$ are distributed according to the range of "up and over" paths arriving at Z in midlatitudes (Figure 1). The exponential decrease in air mass with height causes the contributions to decrease exponentially with maximum path height achieved.

The joint distribution reveals the one-to-one relationship between maximum height Z' and transit time ξ that occurs when there is no mixing between the tropics and the midlatitudes. According to (6) each transit time corresponds to a single maximum height as

$$\xi = \frac{Z'}{W} + \frac{(Z' - Z)}{\alpha W}. \quad (9)$$

This is simply the time required to advect up to Z' in the tropics at rate W and back down to Z in midlatitudes at rate αW. The joint distribution's singular line in the ξ-Z' plane decays in amplitude (area under the delta function) with higher Z' and longer ξ due to the air density exponential decay with height. As there is a one-to-one relationship between Z' and ξ in the nondetraining limit, the age spectrum also decays exponentially with ξ. Changing W simply changes the slope and intercept of the singular line.

3.3. Advection, Detrainment, No Diffusion

Mixing from midlatitudes to the tropics causes recirculation. Particles can cross back and forth between regions before arriving at the parcel under observation. This is shown schematically in Figure 2a , and the effect on the joint distribution is shown in Figure 2b. With recirculation it is possible for two paths to achieve the same maximum path height but have different transit times (or the same transit time but different maximum path heights), so that the singular line in the ξ-Z' plane for the nondetraining limit now becomes a 2-D distribution. As will be demonstrated below, this 2-D distribution consists of a singular line positioned as in the nondetraining case and a distributed component falling exclusively below the singular line. For a particular transit time the highest height achieved is by a direct (nonrecirculated) path. Recirculation always results in lower maximum heights.

The analytic solution for the advective-detraining age spectrum is presented in Appendix A, and examples for different rates of mixing between the midlatitudes and the tropics are shown in Figure 3 . The age spectrum in the tropics contains a lagged delta function as in the nondetraining limit. However, comparison of equations (3) and (A1) reveals that now the delta function magnitude is diminished exponentially with Z, as a progressively smaller fraction of tropical air has come directly from the tropical tropopause compared to air that has been mixed into the tropics from midlatitudes. This diminished pure advective contribution is compensated by a spectral "tail" due to the older midlatitude air. The age spectrum in midlatitudes has a step function at $\xi = Z/W$, as in the nondetraining limit. However, the tail region is elongated. At high rates of mixing the tropical spectral tail becomes a broad, secondary spectral peak (Figure 3a at $Z = 3H$), and the peak of the midlatitude spectrum moves away from the advective time Z/W (Figure 3a at $Z = 2H$ and $3H$ and Figure 3b at $Z = 3H$). The singularity in G_T and discontinuity in G_M may at first seem perverse, given that 2-D and 3-D numerical models show nothing of the sort [*Hall and Waugh*, 1997a]. However, as will be seen below, small amounts of diffusion are sufficient to suppress the

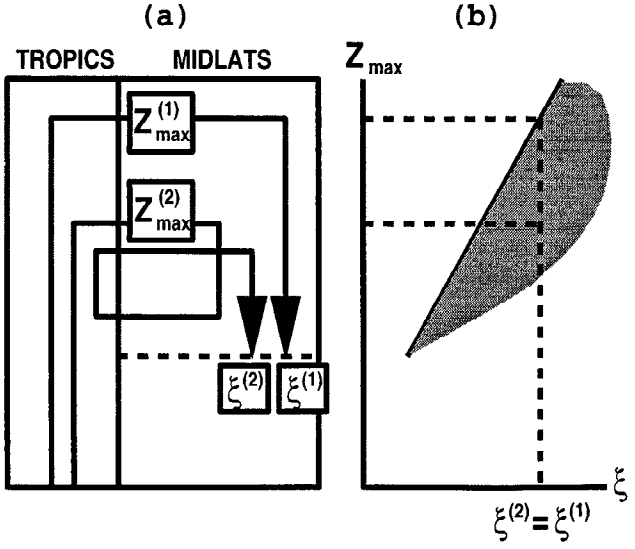

Figure 2. As in Figure 1 but now with detrainment, which allows for recirculation.

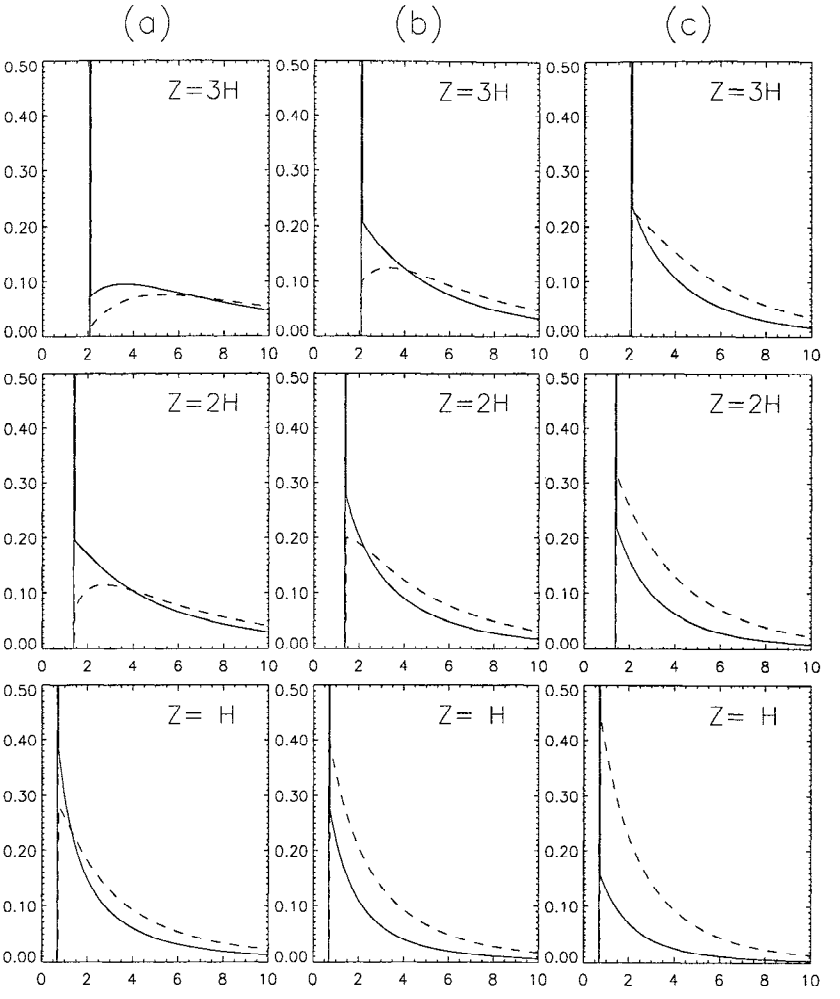

Figure 3. Tropical (solid) and midlatitude (dashed) age spectra for the nondiffusive detraining case with $W = 0.3$ mm/s and $\alpha = 0.5$: (a) $\tau = 0.5$ year, (b) $\tau = 1$ year, and (c) $\tau = 2$ years. In each column the three panels correspond to $Z = H$, $2H$, and $3H$, as labeled. The horizontal axes are transit time in years, and the vertical axes are spectral density in years^{-1}.

singularity and discontinuity, even while the "tail" of the spectrum remains dominated by the recirculation.

Age spectra alone do not provide information on where the recirculated air has been. However, the joint distribution provides a way to distinguish the different paths that have identical transit times. I was not able to obtain $\mathcal{P}$ analytically in the detraining case (the Laplace transform of the solution is readily obtained, but I was not able to perform the inversions), but direct numerical integration of (1) and (2) is possible. Examples are shown in Figure 4 for the midlatitude lower stratosphere and for several values of τ. The corresponding age spectra and MPH distributions are plotted below and to the right of each $\mathcal{P}$, and the mean age and "mean maximum path height" (see section 4) are indicated by dashed lines. As τ is increased, $\mathcal{P}$ approaches the singular distribution of (6), in which each transit time corresponds to a unique maximum height. For finite τ the singular line is still present (but kept finite in Figure 4 by the limitations of numerical integration), representing the direct advective (nonrecirculated) "up and over" path, which is the maximum path height available for a given ξ. Now, however, for each ξ, recirculation causes a broad distribution of lower maximum path heights, compensating the amplitude of the singular line, which is reduced compared to the nondetraining limit. Note that for a given transit time, midlatitude-tropical mixing causes recirculation that results in maximum path heights always lower than they would be otherwise.

Although I have not obtained $\mathcal{P}$ analytically, the MPH distribution can be obtained directly from (1) and (2) according to the recipe of section 2, yielding

$$\mathcal{Z}_T(Z,Z') = \frac{1}{H}\epsilon_+ e^{Z'/H}\frac{(e^{Z/H}-1)}{(e^{Z'/H}-\epsilon_+)^2}\,\Theta(Z'-Z) + \frac{(e^{Z'/H}-\epsilon_+ e^{Z/H})}{(e^{Z'/H}-\epsilon_+)}\,\delta(Z'-Z), \quad (10)$$

$$\mathcal{Z}_M(Z,Z') = \frac{1}{H}e^{Z'/H}\,\frac{(e^{Z/H}-\epsilon_+)}{(e^{Z'/H}-\epsilon_+)^2}\,\Theta(Z'-Z), \quad (11)$$

where $\epsilon_+ = \epsilon/(1+\epsilon)$. Examples are shown in Figure 4 to the right of $\mathcal{P}$ in each panel. Notice that $\mathcal{Z}_M$ varies

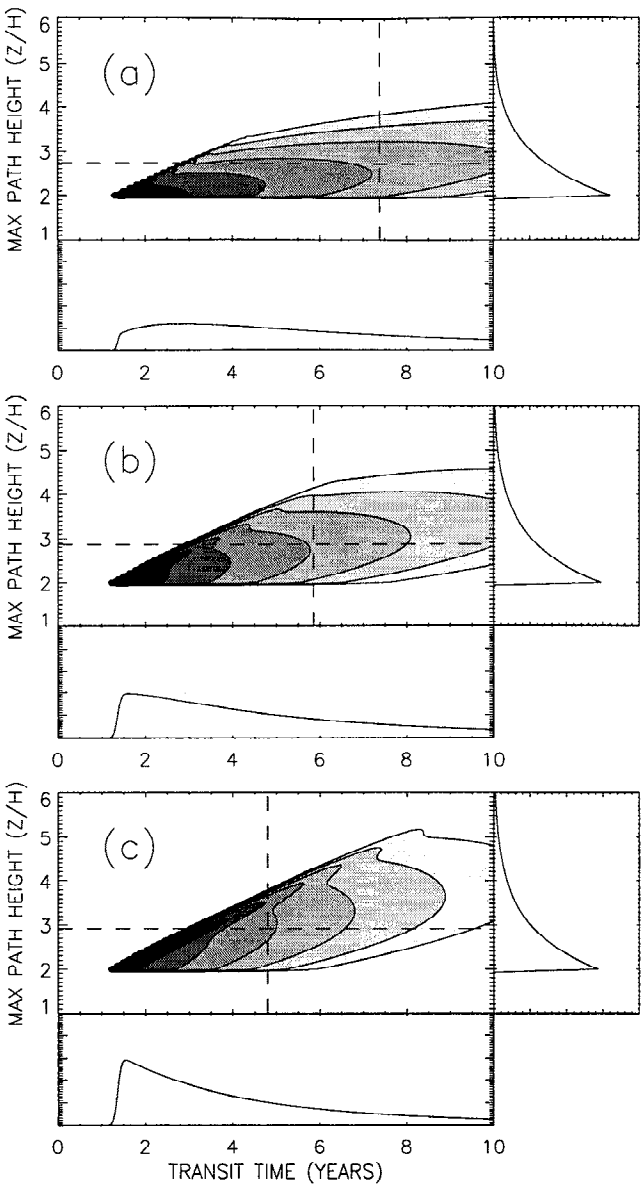

Figure 4. Joint distribution, maximum path height (MPH) distribution, and age spectrum in midlatitudes ($\mathcal{Z} = 2H$) for the nondiffusive detraining case with $W = 0.3$ mm/s and $\alpha = 0.5$. (a) $\tau = 0.5$ year, (b) $\tau = 1$ year, and (c) $\tau = 2$ years. In each panel the gray scale contour plot is $\mathcal{P}$, the plot below it is G, and the plot to the right is $\mathcal{Z}$. Contour levels for $\mathcal{P}$ decrease by factors of 2 from black to white, for a total factor range of 128. The dashed curves indicate the mean age and mean maximum path height.

only weakly with τ (via ϵ) compared to the strong τ dependence of G seen in Figure 3. I return to this in section 4.

3.4. Advection, Detrainment, Diffusion

With vertical diffusion present in the TLP model, analytic expressions for G and $\mathcal{P}$ are no longer available, and the age spectra and joint distributions are computed numerically. (However, $\mathcal{Z}$ may still be obtained analytically; a quantity related to it is presented in Appendix B.) Vertical diffusivities typical of observationally based estimates, ~ 0.1 m^2/s [*Hall and Waugh*, 1997b; *Sparling et al.*, 1997; *Mote et al.*, 1998], do not change the picture qualitatively, although the advective singularities and step functions of the nondiffusive distributions (Figures 3 and 4) are smoothed. Figure 5 repeats the age spectra shown in Figure 3, but now with $K = 0.5$ m^2/s in both the tropical and midlatitude regions, a value probably typical in many 2-D and 3-D numerical models of total effective diffusion due to resolved waves, explicit parameterization, and numerical formulation. The resulting spectra are reminiscent of age spectra from 2-D and 3-D models [*Hall and Waugh*, 1997a; *Park et al.*, 1999]. Note that the age spectral tail remains dominated by recirculation, suggesting that much of the information provided by analysis of the full TLP model is contained in the nondiffusive TLP model, which is easier to treat analytically. Figure 6 shows G_M, $\mathcal{P}_M$, and $\mathcal{Z}_M$ (as in Figure 4) for $\tau = 1$ year and $K = 0.5$ m^2/s.

3.5. Particle Calculations

The distributions G, $\mathcal{P}$, and $\mathcal{Z}$ represent Eulerian descriptions of Lagrangian path statistics. This type of information and more can also be computed from direct Lagrangian particle simulations [*Schoeberl et al.*, 2000; *Eluszkiewicz et al.*, 2000]. Eulerian diagnostics, however, have several advantages: (1) They implicitly incorporate all the mixing natural to the system; (2) an Eulerian tracer completely samples all transport paths, regardless of variations in background fluid density, whereas statistical convergence with Lagrangian particles may require an enormous surplus of particles in high-density regions in order to sample low-density regions sufficiently. (For this reason, *Eluszkiewicz et al.* [2000] did not include the troposphere in their 3-D particle mean age simulations.) Nonetheless, the language used to discuss the distributions ("paths" and "transit times") is the language of particles. Therefore it is worthwhile verifying the interpretation of G, $\mathcal{P}$, and $\mathcal{Z}$ with direct particle statistics. I used the TLP model to compute particle back-trajectories, accounting for the mixing between adjacent latitude regions by providing a probability $\Delta t/\tau$ at each time step Δt for a particle to switch regions. Figure 7 shows the age spectrum and MPH distribution for the advective-detraining case computed analytically, by numerical integration of equations (1) and (2), and by binning of Lagrangian particles by transit time and maximum path height. The agreement is good, after allowing for statistical fluctuations of the particle analysis and numerical diffusion of the advection algorithm (second-order moments [*Prather*, 1986]). This confirms the Lagrangian statistical interpretations of G, $\mathcal{P}$, and $\mathcal{Z}$.

3.6. Three-Dimensional Numerical Model

The TLP model is idealized. To help verify that insights gained from it are relevant to the stratosphere, it is worthwhile observing the distributions in a more realistic setting. Figure 8 shows the joint distribution, age

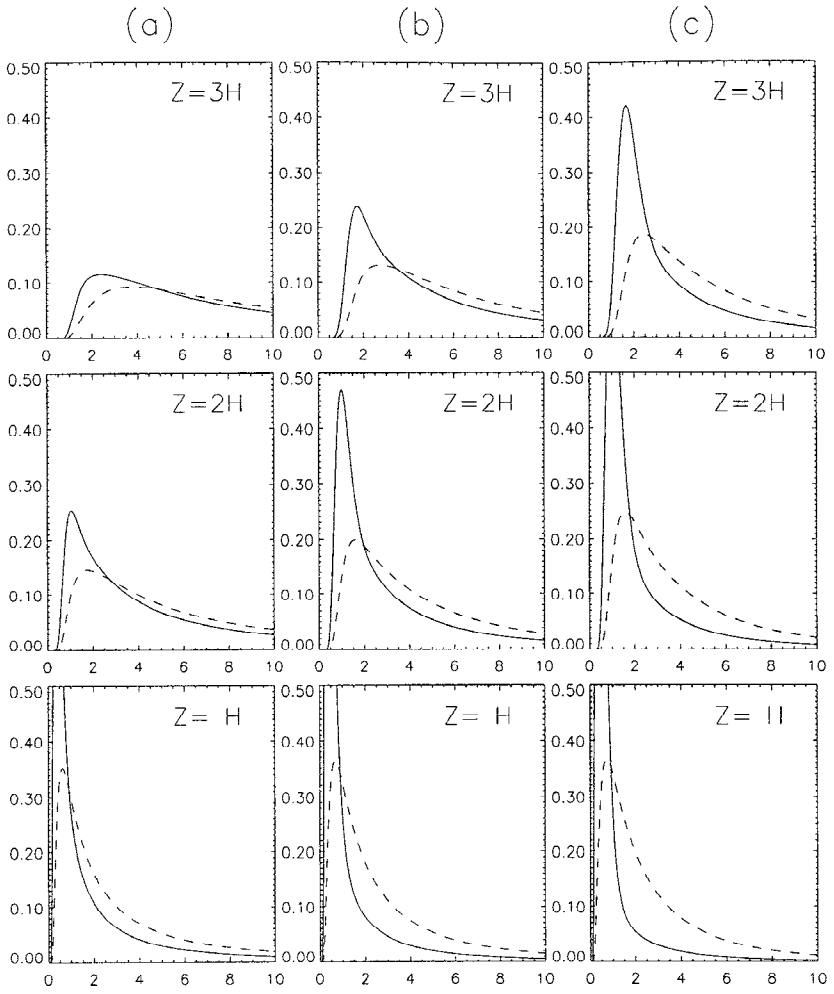

Figure 5. As in Figure 3 but with $K = 0.5$ m^2/s.

spectrum, and MPH distribution in the lower midlatitude stratosphere of a 3-D chemical transport model (CTM) [*Prather et al.*, 1987] driven by a repeated year of wind data from the middle-atmosphere GCM of the Goddard Institute for Space Studies. The low-resolution version of the GCM is used here, having 21 layers, with 12 in the stratosphere and mesosphere, and a horizontal resolution of 8° by 10° [*Rind et al.*, 1988]. Evident in Figure 8 are oscillations due to seasonality in transport that is not included in the TLP model. In addition, because the tropical upwelling in this GCM is more rapid than the observationally based 0.3 mm/s used for the TLP model in Figures 4 and 6, the slope of the leading edge of the GCM joint distribution is steeper. Overall, however, the morphology of the distributions are similar, lending credibility to the TLP-based interpretations. Future studies are planned to compare the joint and MPH distributions among different GCMs.

4. Mean Age Maximum Path Height Relationship

A feature revealed by this analysis is the very different dependence of the age spectrum and the MPH distribution on rates of large-scale stratospheric transport processes. Comparing the cases of slow mixing (Figure 4a) and rapid mixing (Figure 4c), one sees that the midlatitude age spectrum is significantly "stretched" by the mixing, while the MPH distribution has varied relatively little (see also Figures 9a and 9b). To examine and compare these different sensitivities in more detail, it is useful to have measures that summarize the distributions. The first moment, the mean age, is a natural measure of G, as it may be inferred from observations. For the TLP model with $K = 0$, it is

$$\Gamma_T(Z) = (1 + \frac{\epsilon}{\alpha_+})\frac{Z}{W}, \tag{12}$$

$$\Gamma_M(Z) = (1 + \frac{\epsilon}{\alpha_+})\frac{Z}{W} + \frac{1}{\alpha_+}\frac{H}{W}, \tag{13}$$

where $\alpha_+ = \alpha/(1 + \alpha)$. (See Appendix B for the case with midlatitude vertical diffusion and Appendix C for spatial variation in W. Also see *Neu and Plumb* [1999] for more general expressions, including both midlatitude and tropical vertical diffusion, as well as differing tropical and midlatitude tropopause height.)

Various measures of the MPH distribution are possible. In analogy to the mean age, the first moment of the

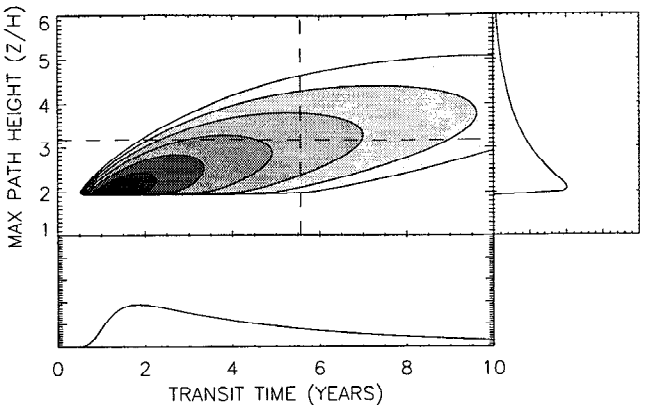

Figure 6. As in the Figure 4b but with $K = 0.5$ m^2/s.

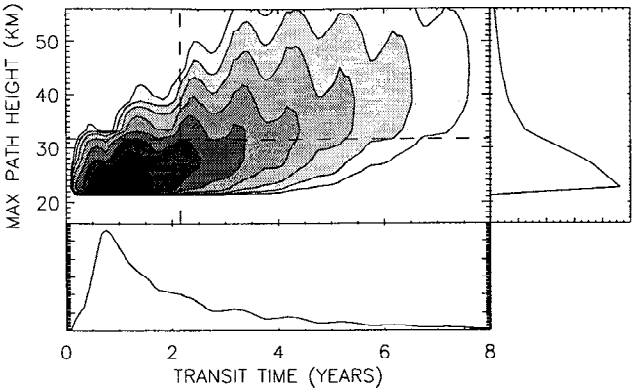

Figure 8. Distributions $\mathcal{P}$, $\mathcal{Z}$, and G in the GISS 3-D chemical transport model (CTM) at the height 22 km and latitude 44°N. Contour levels as in Figure 4.

MPH distribution is the "mean maximum path height" $\overline{\mathcal{Z}} = \int_Z^\infty Z' \mathcal{Z}(Z, Z')dZ'$. For the advective-detraining case with no diffusion,

$$\overline{\mathcal{Z}}_T(Z) = Z + H(e^{Z/H} - 1) \ln\left(\frac{e^{Z/H}}{e^{Z/H} - \epsilon_+}\right), \quad (14)$$

$$\overline{\mathcal{Z}}_M(Z) = Z + \frac{H}{\epsilon_+}(e^{Z/H} - \epsilon_+) \ln\left(\frac{e^{Z/H}}{e^{Z/H} - \epsilon_+}\right), \quad (15)$$

where $\epsilon_+ = \epsilon/(1 + \epsilon)$. For $\epsilon = 0$ (the nondetraining limit), $\overline{\mathcal{Z}}_T = Z$ and $\overline{\mathcal{Z}}_M = Z + H$, which are the first moments of (7) and (8), respectively. Note that the mean maximum path height is not the same as the maximum height of the mean path defined by *Schoeberl et al.* [2000]. Using a zonally averaged model, *Schoeberl et al.* [2000] computed the time-dependent center of mass position of many particle back-trajectories to the tropopause. The resulting mean path has a maximum height at a particular time, but most particles will not have their individual maxima at that time. By contrast, the mean maximum path height, as defined here, is the mean over each particle maximum, independent of when the maximum was achieved. The mean maximum path height is always greater than the maximum height of the mean path.

The mean MPH in midlatitudes is shown in Figures 4 and 6 for the TLP model with various values of τ. As will be discussed below, $\overline{\mathcal{Z}}$ depends only weakly on the mixing timescale τ. Figure 9a shows the zonal-mean annual-mean $\overline{\mathcal{Z}}$ for the 3-D CTM. For example, at 22 km in the tropics, $\overline{\mathcal{Z}} \approx 25$ km, while at 22 km in high latitudes, $\overline{\mathcal{Z}} \approx 35$ km. The zonal-mean $\overline{\mathcal{Z}}$ countours display characteristics typical of stratospheric long-lived tracers and are similar in orientation to this model's distribution of N_2O and mean age [*Hall and Prather*, 1995]. Note that the midlatitude contour orientation is not subject to analysis by the TLP model. (In the TLP formulation, one assumes a midlatitude contour orientation universal to long-lived tracers and uses these parallel contours as the 1-D coordinate [*Plumb*, 1996; *Neu and Plumb*, 1999].) The statements that follow about relative sensitivities to transport rates of mean age and mean MPH, based on the TLP model analysis, refer to magnitudes and vertical structure of the quantities in the midlatitudes and tropics. Vertical $\overline{\mathcal{Z}}$ profiles for the 3-D CTM at the equator and 45°N are shown in Figure 9b and are qualitatively similar in their height dependence to the TLP results (equations (14) and (15)), having only a weak deviation from a slope of unity but with a shift.

As an alternative measure of $\mathcal{Z}$, one can consider $F(Z, Z') = \int_{Z'}^\infty \mathcal{Z}(Z, Z'')dZ''$, the mass fraction of the

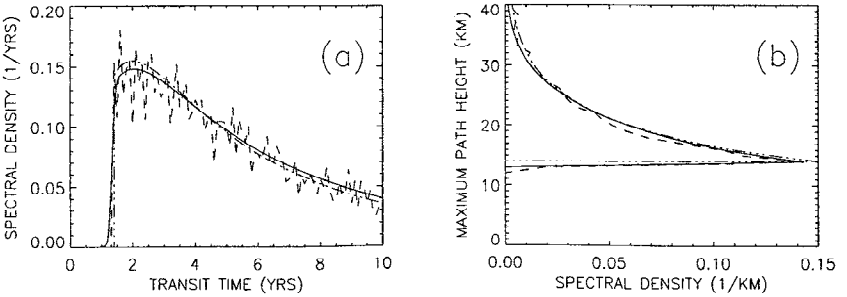

Figure 7. (a) G_M with $Z = 2H$, $K = 0$, $W = 0.3$ mm/s, $\alpha = 0.5$, and $\tau = 0.75$ years computed analytically (dotted-dashed line), by numerical integration of the tropical leaky pipe (TLP) equations (solid line), and by binning of Lagrangian particles (dashed line). (b) $\mathcal{Z}_M$ by the same three methods.

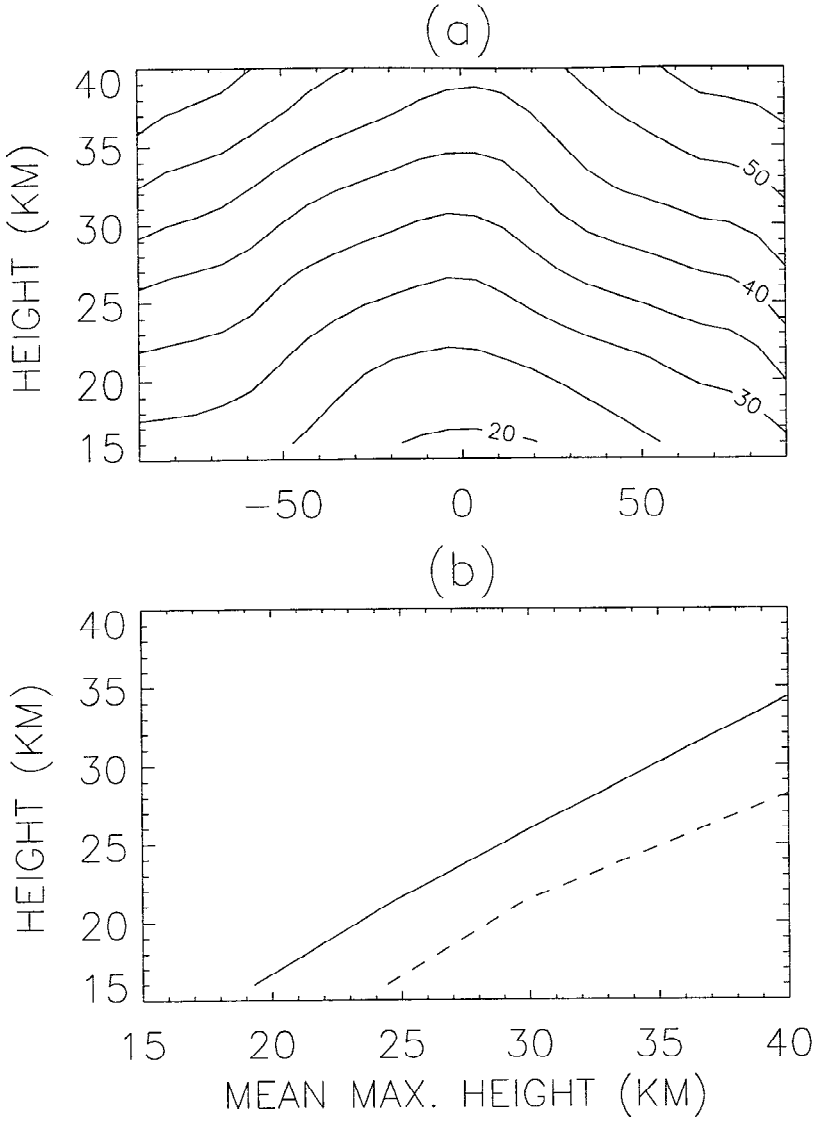

Figure 9. (a) Zonal-mean annual-mean contours of mean MPH for the 3-D CTM. Contours are labeled in kilometers. (b) Vertical profiles at the equator (solid) and 45°N (dashed).

parcel at Z that has passed above Z'. (For example, $Z' = Z + H$ would be a natural choice.) For the TLP with $K = 0$, one finds, either directly from (1) and (2) or from integration of (10) and (11),

$$F_T(Z, Z') = \epsilon_+ \frac{e^{Z/H} - 1}{e^{Z'/H} - \epsilon_+}, \tag{16}$$

$$F_M(Z, Z') = \frac{e^{Z/H} - \epsilon_+}{e^{Z'/H} - \epsilon_+}. \tag{17}$$

Comparison of Γ and $\overline{Z}$, or Γ and F, reveals very different sensitivities to the circulation parameters W, ϵ, and α. First, $\overline{Z}$ and F are independent of α, the measure of the relative size of the tropics. Second, $\overline{Z}$ and F depend on W only through $\epsilon = H/(\tau W)$, while Γ depends separately on W and ϵ. Thus in the nondetraining limit ($\epsilon = 0$), $\overline{Z}$ and F are independent of W, while Γ varies as $1/W$. Third, Γ increases linearly with ϵ (with an offset), and thus with no vertical diffusion, Γ diverges in the global diffuser ($\epsilon = \infty$) limit. (Vertical diffusion keeps Γ finite in this limit; see Appendix B and *Neu and Plumb* [1999].) In contrast, $\overline{Z}_M$ and F_M are only weakly sensitive to ϵ. For $Z = H$, for example, $\overline{Z}_M$ ranges from $Z + H$ to $Z + 0.8H$ as ϵ ranges $0 \rightarrow \infty$. $\overline{Z}_T$ ranges from Z to $Z + 0.8H$, a larger fractional variation; in the nondetraining limit, no air has traveled above the parcel height in the tropics, so air from above the parcel height due to detrainment represents a larger fractional variation. $F_M(Z, Z + H)$ ranges from 0.37 to 0.27 as ϵ ranges $0 \rightarrow \infty$, while $F_T(Z, Z + H)$ ranges from zero to 0.27. These sensitivities to ϵ are shown in Figure 10 .

That $\overline{Z}$ and F are independent of W in the nondetraining limit can be understood by simple mass continuity. Increasing W correspondingly increases the tropical divergence and the subsequent flux to midlatitudes. Thus although the circulation rate increases and Γ decreases, the mass fraction of any parcel that has been above some specified height since last tropospheric contact remains constant.

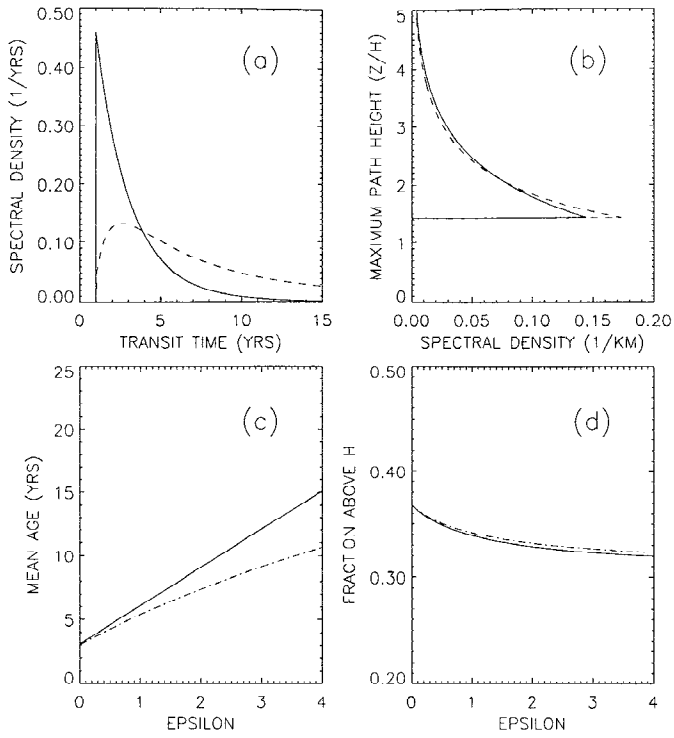

Figure 10. Sensitivity to ϵ in TLP. (a) Nondiffusive G_M at $Z = 2H$ for $\epsilon = 0$ (solid line) and $\epsilon = 3.5$ (dashed curve). (b) Nondiffusive $\mathcal{Z}_M$ at $Z = 2H$ for $\epsilon = 0$ (solid line) and $\epsilon = 3.5$ (dashed curve). (c) Γ_M versus ϵ for no diffusion (solid line) and $K = 0.1$ m^2/s (dotted-dashed line). (d) $F(2H|3H)$ versus ϵ for no diffusion (solid line) and $K = 0.1$ m^2/s (dotted-dashed line). $W = 0.3$ mm/s and $\alpha = 0.5$.

The weak dependence of $\overline{\mathcal{Z}}_M$ and F_M on the tropical-midlatitude mixing, however, seems surprising at first sight. One might expect that the more likely it is for air to recirculate, the more likely it is to sample the full height of the stratosphere. In other words, naively, air that is aged by mixing is air that has been more widely dispersed. This is not the case, however. Physically, the weak sensitivity to mixing can be understood by considering a midlatitude air parcel as follows: If mixing of air from midlatitudes to the tropics increases, than more air is advected upward, ultimately returning to the midlatitude parcel, and the parcel fraction that has been aloft is apparently increased. However, the net mass flux between the tropics and the midlatitudes is constrained by continuity, so with increased mixing, more tropical air must be transported directly out of the tropics to the midlatitude parcel. This air would otherwise have traveled at higher levels, and so the fraction of the parcel that has been aloft is apparently decreased. The two effects of mixing on the midlatitude parcel's MPH distribution oppose each other, and the net result is only a weak dependence on the mixing rate.

These opposing influences are seen in the joint distributions of Figure 4. With increasing mixing (decreasing τ), the MPH distribution at a given Z' is the sum over an increasingly broad range of transit times due to recirculation. However, this is compensated by an increasingly attenuated contribution from the advective singularity. The same argument holds for a tropical parcel. However, whereas a midlatitude parcel has components from aloft even in the nondetraining limit, tropical air has components from aloft due solely to detrainment (for no diffusion), and so the detrainment effect is relatively larger. Compared to $\overline{\mathcal{Z}}$ or F, the mean age Γ is not constrained by continuity in the same way, and increased mixing results in recirculation that directly ages the air in the tropics and midlatitudes. Note, however, that the difference $\Gamma_M - \Gamma_T$ is independent of mixing (for no diffusion) [*Neu and Plumb*, 1999] for reasons similar to $\mathcal{Z}$ and $\mathcal{P}$.

The different transport sensitivities go further. Midlatitude vertical diffusion can significantly decrease the mean age, especially when tropical-midlatitude mixing is rapid. (As noted above, it is diffusion that keeps mean age finite in the instantaneous mixing limit.) The MPH distribution, on the other hand, is only weakly sensitive to diffusion. $F(Z, Z')$ and $\Gamma(Z)$ with detrainment and midlatitude diffusion are presented in Appendix B. The dashed curve in Figure 10 shows the variation of Γ_M and $F_M(Z, Z + H)$ with ϵ for $K = 0.1$ m^2/s. The F_M curves are nearly indistinguishable from the nondiffusive case, while the Γ_M curves are noticeably different. In fact, in a 1-D mass-weighted diffusion model with uniform K, the MPH distribution is independent of K, depending only on the scale height. (This can be seen directly from the steady-state 1-D mass-weighted diffusion equation with boundary conditions but no explicit sources. K multiplies all the terms and simply drops out.) Mean age for the 1-D model, in contrast, is inversely proportional to K [*Hall and Plumb*, 1994].

The diagnostics Γ and F are presented in Appendix C for the nondiffusive advective-detraining case with general spatial variation in W. $F(Z, Z')$ depends on W only through the ratio $W(0)/W(Z')$, so the geometry of the upwelling has consequences for the MPH distribution, but the overall magnitude of the circulation does not. By contrast, the mean age has terms proportional to $1/W(Z)$ and $\int_0^Z dZ'/W(Z')$, and thus both the geometry and the magnitude are important.

5. Summary and Discussion

In this paper the age spectrum has been complemented by the distribution of maximum path height (MPH) in order to obtain information about the path histories of components of a stratospheric air parcel. Taken together, one has a joint distribution of maximum path height and transit time. Using these distributions to analyze the tropical leaky pipe (TLP) model, a model that represents the dominant large-scale transport effects of the time-averaged stratospheric circulation but is simple enough to allow easy physical insight, I obtain relationships between timescales, path histories, and transport rates. The maximum path height of an air parcel component ("particle") varies much less across different representations of the circulation than

its transit time. The age spectrum and the mean age are sensitive to rates of the model's transport processes, namely tropical upwelling, tropical-midlatitude mixing, and vertical diffusion. By contrast, the MPH distribution is much more weakly sensitive to these processes, especially in midlatitudes.

These differing sensitivities help to understand the relationship between mean age and trace gases of known tropospheric concentration and with rapid upper stratospheric photochemistry (e.g., N_2O, CH_4, CFCs, Cl_y). Such gases are constrained from below and above, and therefore their stratospheric concentrations cannot be so sensitive to circulation as mean age, which is constrained below ($\Gamma(0) = 0$) but not above. More concretely, consider the conceptual limit in which a tracer's photochemical lifetime below some height Z_{PC} is long compared to the longest transport timescale of interest and short compared to the shortest timescale above Z_{PC}. A stratospheric air parcel below Z_{PC} is composed of a fraction F of particles that have traveled above Z_{PC} since last tropospheric contact and a fraction $1 - F$ of particles that have not. Particles in the $1 - F$ fraction have mixing ratios dependent on their transit times; the photochemistry is slow along the paths of these particles, no particle's tracer is completely depleted (or saturated, in the case of a gas created in the stratosphere by conversion from another gas of tropospheric origin), and each particle's mixing ratio simply declines (or increases) with increasing photochemical exposure time. In contrast, the particles in fraction F that travel into the rapid photochemistry region above Z_{PC} are completely depleted (or saturated) of tracer, independent of transit time. Nonetheless, if the probability that a particle reached Z_{PC} and the probability that it had a particular transit time had similar sensitivities to transport rates, then, combined with the close relation between mixing ratio and transit time for the lower $1 - F$ fraction, the mixing ratio of the entire parcel (the observable quantity) would depend strongly on the parcel's average transit time, the mean age. However, the TLP analysis presented here indicates that the probability that a particle has passed above any given level is much less sensitive to transport rates than is its transit time; that is, the magnitude of F is not a strong function of the mean age. Unlike mean age, the fraction F is strongly constrained by mass continuity of stratospheric regions, and as a result, F is less sensitive to transport rates than mean age. This robustness prevents gases of predominantly upper stratospheric photochemistry from varying across different realizations of stratospheric circulation as much as mean age.

The fraction of an air parcel that has passed above a given height Z' increases rapidly with the height Z of the parcel itself, as summarized by (16) and (17) for the nondiffusive TLP model. Thus the relationship between mean age and long-lived tracers of predominantly upper stratospheric photochemistry should be correlated most highly in the lower stratosphere. Consider N_2O which has a local photochemical lifetime greater than 50 years in the tropics below 25 km and less than 0.5 year above 35 km [*Brasseur and Solomon*, 1984]. A parcel well below 35 km has only a small fraction from above 35 km, and one expects a high correlation between mean age and N_2O, as is seen in numerical experiments [*Hall et al.*, 1999; *Li and Waugh*, 1999]. A parcel close to 35 km has a large fraction from above 35 km, and according to the TLP analysis, the size of this fraction is not a strong function of the parcel's mean age. (Using expression (17) with $H = 7$ km, $W = 0.3$ mm/s, and $\tau = 1$ year, so that $\epsilon = 0.7$, one has $F_M(20\text{ km}|35\text{ km}) = 0.1$, while $F_M(30\text{ km}|35\text{ km}) = 0.5$, where a tropopause height assumed at 16 km is first subtracted from Z and Z'.) Thus one expects a weaker correlation between the parcel's mean age and its N_2O mixing ratio over a range of circulation realizations at the higher altitude.

It is not surprising that air well depleted (or saturated) photochemically of a trace gas should display little correlation between the trace gas mixing ratio and the mean age. The new information provided by the maximum path height analysis is that the size of the fractional contribution of depleted (or saturated) air to parcels in a region of slow photochemistry is also not closely related to mean age. This observation may ultimately be a consideration in deciding what is a sufficiently realistic mean age distribution for numerical models to simulate accurately the chemical state of the stratosphere. The wide range of mean age simulations [*Hall et al.*, 1999] and the sensitivity to numerical formulations [*Eluszkiewicz et al.*, 2000] suggest that mean age is a difficult quantity to model accurately. Unlike mean age, trace gases with rapid upper stratospheric photochemistry are affected by how high air has been, as well as the time air spends in the stratosphere, in addition to the other factors that determine total photochemical exposure. Therefore according to the arguments presented here, the distributions of these gases should not be so sensitive to inaccuracies in simulated transport as mean age. Generally, this differing sensitivity will be more evident in the middle stratosphere and above where contributions from depleted regions are larger. In the lower stratosphere, *Hall et al.* [1999] found, among the models they studied, a large variation in NO_y and Cl_y which was highly correlated with mean age. Thus improvements in transport as diagnosed by mean age are at present vital to improving the realism of the chemical state of the lower stratosphere in these models.

Appendix A: Age Spectrum for Advection and Detrainment

For the TLP model with uniform advection and detrainment and no vertical diffusion the age spectrum is

$$G_T(Z,\xi) = \epsilon\tilde{\epsilon}\frac{Z}{HT}\,\mathrm{I}_1(\Phi)\,e^{Z/2H}e^{-t_*/\tau}\,\Theta(\xi - Z/W) + e^{Z/2H}e^{-t_*/\tau}\,\delta(\xi - Z/W), \quad \text{(A1)}$$

$$G_M(Z,\xi) = \left(\frac{\tilde{\epsilon}}{\mathcal{T}} \mathrm{I}_1(\Phi) + A\, \mathrm{I}_2(\Phi)\right) \times e^{Z/2H} e^{-t_*/\tau}\, \Theta(\xi - Z/W), \quad \text{(A2)}$$

where

$$\Phi = \frac{2}{\tau}\alpha_+ \tilde{\epsilon}\, \mathcal{T},$$

$$A = 2\alpha_+(1+\epsilon)\frac{Z}{H\mathcal{T}^2}\left(\left(\frac{1+2\alpha_-}{2\alpha_-}\right)\xi - \frac{Z}{2\alpha_+ W}\right),$$

$$\mathcal{T} = \sqrt{\xi^2 - \frac{Z^2}{\alpha W^2} + \frac{\xi Z}{\alpha_- W}},$$

$$t_* = \alpha_+\left(2 + \frac{1}{\epsilon}\right)\left(\xi + \frac{Z}{2\alpha_- W}\right),$$

$\alpha_\pm = \alpha/(1 \pm \alpha)$, $\tilde{\epsilon} = \sqrt{(\epsilon+1)/\epsilon}$, $\epsilon = H/W\tau$, I_n is the modified Bessel function of the order of n, Θ is the Heaviside function, and δ is the Dirac delta function.

Appendix B: Mean Age and Mass Fraction for Advection, Detrainment, and Midlatitude Diffusion

For the TLP model with uniform advection, detrainment, and finite midlatitude vertical diffusion (but no tropical diffusion) the mean age is

$$\Gamma_T(Z) = \frac{\alpha}{\eta}\frac{Z}{W} + \frac{\epsilon}{\eta}(1+\alpha)\frac{Z}{W} - \frac{\epsilon h}{\eta W}(1+\alpha-\kappa)(1-e^{-Z/h}), \quad \text{(B1)}$$

$$\Gamma_M(Z) = \Gamma_T(Z) + \frac{H}{\eta W}(1+\alpha-\kappa)(1-e^{-Z/h}), \quad \text{(B2)}$$

as adapted from *Neu and Plumb* [1999]. The mass fraction of a parcel at Z that passed above Z' is

$$F_T(Z,Z') = \epsilon_+ \frac{\eta e^{Z/H} + \kappa e^{-Z/h} - \beta}{\eta e^{Z'/H} - \epsilon_+\alpha e^{-Z'/h} - \epsilon_+\beta}, \quad \text{(B3)}$$

$$F_M(Z,Z') = \frac{\eta e^{Z/H} - \epsilon_+\kappa e^{-Z/h} - \epsilon_+\beta}{\eta e^{Z'/H} - \epsilon_+\alpha e^{-Z'/h} - \epsilon_+\beta}, \quad \text{(B4)}$$

where $\beta = \epsilon\kappa + \alpha - \kappa$, $\eta = \epsilon\kappa + \alpha$, $\kappa = K/(WH)$, $\epsilon_+ = \epsilon/(\epsilon+1)$, $\epsilon = H/(W\tau)$, and $h = \kappa H/\eta$ is the thickness of the diffusive boundary layer above the midlatitude tropopause. The MPH distribution may be obtained as $\mathcal{Z}(Z,Z') = -\partial F/\partial Z'$.

Appendix C: Spatial Variation in W

For the TLP model with spatially varying advection, uniform ϵ (detrainment to entrainment ratio), and no diffusion the mean age is

$$\Gamma_T(Z) = \int_0^Z \frac{dZ'}{W(Z')} + \frac{\epsilon}{\alpha_+}\int_0^Z \frac{dZ'}{W(Z')} + \frac{\epsilon}{\alpha_+}\left(\frac{1}{W(Z)} - \frac{1}{W(0)}\right)H, \quad \text{(C1)}$$

$$\Gamma_M(Z) = \Gamma_T(Z) + \frac{1}{\alpha_+}\frac{H}{W(Z)}. \quad \text{(C2)}$$

Neu and Plumb [1999] derived (C2) and discussed the independence of $\Gamma_M - \Gamma_T$ from ϵ. The mass fraction of a parcel at Z that passed above Z' is

$$F_T(Z,Z') = \epsilon_+ \frac{\tilde{w}(Z)e^{Z/H} - 1}{\tilde{w}(Z')e^{Z'/H} - \epsilon_+}, \quad \text{(C3)}$$

$$F_M(Z,Z') = \frac{\tilde{w}(Z)e^{Z/H} - \epsilon_+}{\tilde{w}(Z')e^{Z'/H} - \epsilon_+}, \quad \text{(C4)}$$

where $\tilde{w}(Z) = W(0)/W(Z)$ and $\epsilon_+ = \epsilon/(\epsilon+1)$.

Acknowledgments. I thank Lynn Sparling, Darryn Waugh, Fred Moore, and Mark Holzer for conversations related to this work. This work is supported by the NASA Atmospheric Effects of Aviation Program project NAG5-7138.

References

Andrews, A. E., K. A. Boering, B. C. Daube, S. C. Wofsy, E. J. Hintsa, E. M. Weinstock, and T. P. Bui, Empirical age spectra for the lower stratosphere from in situ observations of CO_2: Implications for stratospheric transport, *J. Geophys. Res.*, *104*, 26,581–26,595, 1999.

Boering, K. A., S. C. Wofsy, B. C. Daube, H. R. Schneider, M. Loewenstein, and J. R. Podolske, Sratospheric mean ages and transport rates derived from observations of CO_2 and N_2O, *Science*, *274*, 1340–1343, 1996.

Brasseur, G., and S. Solomon, *Acronomy of the Middle Atmosphere*, D. Reidel, Norwell, Mass., 1984.

Elkins, J. W., et al., Airborne gas chromatograph for in situ measurements of long-lived species in the upper troposphere and lower stratosphere, *Geophys. Res. Lett.*, *23*, 347–350, 1996.

Eluszkiewicz, J., R. S. Hemler, J. D. Mahlman, L. Bruhwiler, and L. Takacs, Sensitivity of age-of-air calculations to the choice of advection scheme, *J. Atmos. Sci.*, in press, 2000.

Grant, W. B., E. V. Browell, C. S. Long, L. L. Stowe, R. G. Grainger, and A. Lambert, Use of volcanic aerosols to study the tropical stratospheric reservoir, *J. Geophys. Res.*, *101*, 3973–3988, 1996.

Hall, T. M., and R. A. Plumb, Age as a diagnostic of stratospheric transport, *J. Geophys. Res.*, *99*, 1059–1070, 1994.

Hall, T. M., and M. J. Prather, Seasonal evolutions of N_2O, O_3, and CO_2: Three-dimensional simulations of stratospheric correlations, *J. Geophys. Res.*, *100*, 16,699–16,720, 1995.

Hall, T. M., and D. W. Waugh, Timescales for the strato-

spheric circulation derived from tracers, *J. Geophys. Res.*, *102*, 8991–9001, 1997a.

Hall, T. M., and D. W. Waugh, Tracer transport in the tropical stratosphere due to vertical diffusion and horizontal mixing, *Geophys. Res. Lett.*, *24*, 1383–1386, 1997b.

Hall, T. M., and D. W. Waugh, Stratospheric residence time and its relationship to mean age, *J. Geophys. Res.*, *105*, 6773–6782, 2000.

Hall, T. M., D. W. Waugh, K. A. Boering, and R. A. Plumb, Evaluation of transport in stratospheric models, *J. Geophys. Res.*, *104*, 18,815–18,839, 1999.

Harnisch, J., R. Borchers, P. Fabian, and M. Maiss, Tropospheric trends for CF_4 and C_2F_6 since 1982 derived from SF_6 dated stratospheric air, *Geophys. Res. Lett.*, *23*, 1099–1102, 1996.

Holzer, M., and T. M. Hall, Transit-time and tracer-age distributions in geophysical flows, *J. Atmos. Sci.*, in press, 2000.

Johnson, D. G., K. W. Jucks, W. A. Traub, K. V. Chance, G. C. Toon, J. M. Russell, and M. P. McCormick, Stratospheric age spectra derived from observations of water vapor and methane, *J. Geophys. Res.*, *104*, 21,595–21,602, 1999.

Li, S., and D. W. Waugh, Sensitivity of mean age and long-lived tracers to transport coefficients in two-dimensional models, *J. Geophys. Res.*, *104*, 30,559–30,569, 1999.

Minschwaner, K., A. E. Dessler, J. W. Elkins, C. M. Volk, D. W. Fahey, M. Lowenstein, J. R. Podolske, A. E. Roche, and K. R. Chan, The bulk properties of isentropic mixing into the tropics in the lower stratosphere, *J. Geophys. Res.*, *101*, 9433–9439, 1996.

Mote, P. W., T. J. Dunkerton, M. E. McIntyre, E. A. Ray, and P. H. Haynes, Vertical velocity, vertical diffusion, and dilution by midlatitude air in the tropical lower stratosphere, *J. Geophys. Res.*, *103*, 8651–8666, 1998.

Neu, J. L., and R. A. Plumb, The age of air in a leaky pipe model of stratospheric transport, *J. Geophys. Res.*, *104*, 19,243–19,255, 1999.

Park, J., M. K. W. Ko, R. A. Plumb, C. H. Jackman, J. A. Kaye, and K. H. Sage, Report of the 1998 Models and Measurements II Workshop, *NASA Tech. Publ.*, *NASA/TM-1999-209554*, 1999.

Patra, P. K., S. Lal, B. H. Subbaraya, C. H. Jackman, and P. Rajaratnam, Observed vertical profile of sulphur hexafluoride (SF_6) and its atmospheric applications, *J. Geophys. Res.*, *102*, 8855–8859, 1997.

Plumb, R. A., A tropical pipe model of stratospheric transport, *J. Geophys. Res.*, *101*, 3957–3972, 1996.

Prather, M. J., Numerical advection by conservation of second-order moments, *J. Geophys. Res.*, *91*, 6671–6681, 1986.

Prather, M. J., M. B. McElroy, S. C. Wofsy, G. Russell, and D. Rind, Chemistry of the global troposphere: Fluorocarbons as tracers of air motion, *J. Geophys. Res.*, *92*, 6579–6613, 1987.

Rind, D., R. Suozzo, N. K. Balachandran, A. Lacis, and G. Russell, The GISS global climate/middle atmosphere model, I, Model structure and climatology, *J. Atmos. Sci.*, *45*, 329–370, 1988.

Schmidt, U., and A. Khedim, In situ measurements of carbon dioxide in the winter arctic vortex and at midlatitudes: An indicator of the age of stratospheric air, *Geophys. Res. Lett.*, *18*, 763–766, 1991.

Schoeberl, M. R., L. C. Sparling, C. H. Jackman, and E. L. Fleming, A Lagrangian view of stratospheric trace gas distributions, *J. Geophys. Res.*, *105*, 1537–1552, 2000.

Sparling, L. C., and G. H. Weiss, Some effects of beam thickness on photon migration in a turbid medium, *J. Mod. Opt.*, *40*, 841–859, 1993.

Sparling, L. C., J. A. Kettleborough, P. H. Haynes, M. E. McIntyre, J. E. Rosenfield, M. R. Schoeberl, and P. A. Newman, Diabatic cross-isentropic dispersion in the lower stratosphere, *J. Geophys. Res.*, *102*, 25,817–25,829, 1997.

Volk, C. M., et al., Quantifying transport between the tropical and mid-latitude lower stratosphere, *Science*, *272*, 1763–1768, 1996.

Waugh, D. W., et al., Three-dimensional simulations of long-lived tracers using winds from MACCM2, *J. Geophys. Res.*, *102*, 21,493–21,513, 1997.

T. M. Hall, NASA Goddard Institute for Space Studies, 2880 Broadway, New York, NY 10025. (thall@giss.nasa.gov)

(Received February 10, 2000; revised May 1, 2000; accepted May 16, 2000.)